PHYSICAL REVIEW B VOLUME 43, NUMBER 14 15 MAY 1991-I

Gradient-corrected density functionals: Full-potential calculations for iron

D. J. Singh and W. E. Pickett
Complex Systems Theory Branch, Naval Research Laboratory, Washington, D.C. 20375-5000

H. Krakauer
Department of Physics, College of William and Mary, Williamsburg, Virginia 23185

(Received 16 November 1990)

Full-potential calculations of the electronic structure and ground-state properties of iron using the Langreth-Mehl-Hu, Perdew-Wang, and Becke gradient-corrected local-density functionals are reported. As in earlier linear-muffin-tin-orbital calculations using the atomic-spheres approximation, a ferromagnetic bcc ground state is found, although there are differences in the energetics. The effect of the gradient corrections on the electronic structure is discussed in detail. It is found that there are significant changes in the exchange splittings that result from nonspherical terms in the potential, and these differ significantly depending on the choice of the gradient correction.

INTRODUCTION

It is now well established that the local (spin-) density approximation (LSDA) provides an accurate and computationally tractable theoretical framework for calculations of ground-state properties of a wide range of materials. The local approximation is, however, not without certain deficiencies. In addition to its poor description of the properties of highly correlated systems, such as Mott insulators and certain f-band materials, important deficiencies in the LSDA have been found for $3d$ metals (see, for example, Refs. 1–5). Of these, perhaps the most notable is the LSDA's incorrect prediction of a close-packed ground state for iron.[1-3,6] In the hope of correcting these and other deficiencies of the LSDA, there has been considerable interest in nonlocal density functionals, such as the weighted-density approximation[7,8] and gradient-corrected (GC) local (spin-) density approximations.[9-12] In this study we focus on GCLSDA.

Based on an analysis of the failure of direct gradient expansions of the exchange-correlation (xc) functional to improve the LDA, Langreth and Mehl[10] proposed a modified gradient expansion and found that its use improved the ground-state properties of atoms. Since then, Perdew and co-workers[11] and Becke[12] have proposed alternate functionals. Subsequent calculations have shown that the use of GCLSDA improves the ground-state properties of many atomic and molecular systems.[12-18] Lagowski and Vosko,[18] however, found that the improvements were less dramatic for $3d$ atoms than for lighter atoms.

In addition to the calculations on atoms and molecules, a limited number of calculations have been reported for solids using GCLDA.[19-23] For nonmagnetic systems, relatively small changes in the electronic structures and ground-state properties were found. In some cases these changes improved the agreement with experiment. In others, however, the agreement was found to be degraded. One consistent change effected by the inclusion of GC's is a small increase in the lattice parameter, which in many cases improves agreement with experiment. For the magnetic systems that have been studied, the changes are more dramatic, particularly in the case of iron for which a ferromagnetic bcc ground state is predicted.[21,22] Unfortunately, in addition to the improved ground state, changes in the exchange splittings were found which degraded the agreement with experiment, although as shall be shown below these are strongly modified when a full-potential approach is used. On a related noted, Kutzler and Painter[15] have performed calculations for atoms and find that GCLSDA stabilizes nonspherical atoms. This is in contrast to the result using the LSDA where even in those cases where nonspherical solutions are found, the energy gain due to the asphericity is small. As will be discussed in more detail below, this is significant because it has been argued that certain deficiencies of the LSDA in magnetic solid-state systems could be corrected by a more anisotropic xc potential.[25,26]

Here we report general-potential linearized augmented plane-wave[27] (LAPW) calculations for iron using the Langreth-Mehl-Hu (LM), Perdew-Wang (PW), and Becke GCLSDA functionals. These are, to our knowledge, the first full-potential GCLSDA calculations reported for a transition metal and the first calculations for iron using the Becke exchange only functional. Detailed electronic structures are reported and the effect of non-muffin-tin contributions is discussed.

METHOD

As mentioned, the total-energy calculations reported here were performed using a general-potential LAPW method. This method has been discussed in detail previously.[27] Accordingly, only those aspects particular to the present study are discussed here. In the LAPW method the second derivatives of the basis functions are not continuous at the sphere boundaries. Consequently, the charge densities also have discontinuities in their second

©1991 The American Physical Society

derivatives. Since, unlike the case for the LSDA, the GCLSDA xc potentials depend on second derivatives of the charge density, discontinuities in the potential can (and do) occur with the LAPW method at the sphere boundaries. In view of the purpose of the present study, which is to investigate in detail effects due to changes in the xc potentials, we felt that it was important to control this potential source of error. Accordingly, some calculations were performed using a superlinearized augmented plane-wave (SLAPW) method in which continuity of second derivatives is enforced at the sphere boundaries.[28] Tests indicated that enforcing continuity in this way yields only small changes in the results.

The calculations reported here were performed using an iron sphere radius of $R_{\mathrm{MT}}=2.05$ a.u. and basis-set cutoffs of $R_{\mathrm{MT}}K_{\max}=9.0$ and 10.25 for the LAPW and SLAPW calculations, respectively. Total-energy calculations were performed for a range of lattice parameters between 5.10 and 5.45 a.u. for the bcc structure and between 6.0 and 6.6 a.u. for the fcc structure. Static lattice ground-state properties were extracted from these calculations using fits to the Murnaghan equation of state.[29] The Brillouin zone averages in these self-consistent calculations were performed using 60 special **k** points[30] for the fcc structure and 40 for the bcc structure. Convergence tests indicated that these choices yield well-converged total energies. On the other hand, they also indicated that the calculated magnetic moment of bcc iron was somewhat underconverged with this sampling and, accordingly, for the calculation of the magnetic properties, a set of 240 special **k** points was used.

CALCULATION OF xc ENERGIES AND POTENTIALS

The LSDA calculations reported here were performed using the von Barth–Hedin (vBH) form of the xc function.[31] Explicit functional forms for the LM and PW xc potentials in terms of the spin densities, ρ_σ, are given in Refs. 15 and 11, respectively. The form of the xc potential, $v_{\mathrm{xc},\sigma}$, for the Becke GCLSDA functional may be obtained using the Euler-Lagrange equation, as follows:

$$v_{\mathrm{xc},\sigma}=v^{\mathrm{LSD}}_{\mathrm{xc},\sigma}+\frac{\partial L}{\partial\rho_\sigma}-\frac{d}{dx}\left[\frac{\partial L}{\partial(\partial\rho_\sigma/\partial x)}\right]-\frac{d}{dy}\left[\frac{\partial L}{\partial(\partial\rho_\sigma/\partial y}\right]-\frac{d}{dz}\left[\frac{\partial L}{\partial(\partial\rho_\sigma/\partial z)}\right], \tag{1}$$

where $v^{\mathrm{LSD}}_{\mathrm{xc},\sigma}$ is the LSDA xc potential for spin σ. L is given by

$$L=\beta\rho_\sigma^{4/3}\frac{\alpha_\sigma^2}{[1+6\beta\alpha_\sigma\sinh^{-1}(\alpha_\sigma)]} \tag{2}$$

and

$$\alpha_\sigma=\frac{|\nabla\rho_\sigma|}{\rho_\sigma^{4/3}}\ . \tag{3}$$

For the calculations using Becke and LM GC's, the vBH form of the local xc function was used, while the parametrization of Perdew and Zunger was used[32] with the PW GC.

Since the GCLSDA energy functionals depend on the gradient of the charge density, calculation of the corresponding potentials requires the evaluation of first and second derivatives of the charge density. In the general-potential LAPW method, space is divided into two regions, nonoverlapping atom-centered, so-called muffin-tin (MT), spheres and the remaining interstitial region. The charge densities and potentials are represented in terms of lattice harmonics tabulated on a radial mesh inside the MT spheres and in terms of symmetrized plane waves outside. For evaluating the xc energies and potentials the charge density is evaluated on numerical meshes. These are the fast Fourier transform mesh outside the spheres and logarithmic radial meshes along a set of rays inside the spheres. The density is then fitted by third-order polynomial forms in the vicinity of each mesh point. (Depending on the region involved, between 27 and 45 nearby mesh points are used in the fits.) The required derivatives are extracted from the coefficients of the polynomials. In the interstitial region an alternate scheme using Fourier transforms to avoid using fits is feasible. Such a scheme was not used here because it is less efficient.

RESULTS

The principal results of our total-energy calculations are given in Tables I and II. The results for the LM and PW GCLSDA functionals are in qualitative agreement with the results of previous linear-muffin-tin-orbital (LMTO) calculations.[21,22] In particular, the ferromagnetic bcc phase is correctly predicted to be the ground state using the LM and PW xc functionals. (We also find that the Becke functional also yields the correct ground state.) The size of the discrepancies between the present full-potential calculations and those of Refs. 21 and 22 is consistent with those which may be expected to result from the neglect of nonspherical contributions in the LMTO calculations.[3]

For all three forms of the GCLSDA an expansion of the lattice with a reduction in the bulk modulus was found, which in the case of iron improves the agreement with experiment. As was found in the study of Ref. 21,

TABLE I. Energetics of iron with the vBH (local) xc function and the LM, PW, and Becke GC xc functionals. *E*(bcc-*F*) denotes the energy (in mRy with respect to the fcc energy) of the bcc phase while *E*(bcc-*P*) is the energy of a hypothetical nonmagnetic bcc phase. E_{mag} is the difference, *E*(bcc-*P*)-*E*(bcc-*F*).

	E(bcc-*P*)	*E*(bcc-*F*)	E_{mag}
vBH	25.8	4.1	21.7
LM	24.7	−6.8	31.5
PW	21.2	−13.9	35.1
Becke	23.3	−9.0	32.3
LM (LMTO)[a]	22	−3	25
PW (LMTO)[a]	23	−11	34

[a] Reference 21.

TABLE II. Ground-state properties of ferromagnetic bcc iron. Here a is the lattice parameter, B the bulk modulus, B' its pressure derivative, and M the spin moment (per atom) at the experimental lattice parameter.

	a (Å)	B (GPa)	B'	M
vBH	2.76	251	3.1	2.194
LM	2.80	243	3.0	2.263
PW	2.88	182	3.1	2.127
Becke	2.86	202	3.1	2.185
PW (LMTO)[a]	2.88	170		2.30
Expt.	2.86	172		2.12

[a] References 21 and 22.

this expansion is larger for the PW functional than for the LM functional. The lattice parameter calculated using the Becke functional is very close to that calculated using the PW functional, although the bulk modulus is significantly larger. This is an indication that the softening of the bulk modulus when GC xc functionals are used is not just a result of the expansion of the lattice. In fact, in all three cases the calculated bulk modulus is larger than that which would be expected from the expansion of the lattice and the vBH values of B and B'. The best agreement with the experimental structural properties is obtained using the PW functional.

As may be noted from Table I, only small changes in the paramagnetic fcc-bcc energy difference result when GC's to the LSDA are used. The stabilization of the bcc phase arises almost entirely from an enhancement of the magnetic energy. This is consistent with the small changes found in previous GCLSDA calculations for nonmagnetic materials. It is notable that in spite of the increase in magnetic energy, the present calculations do not show significant enhancements of the magnetization over the LSDA result and, in fact, for the PW and Becke GC xc functionals, reductions are found. This is in contrast to the increase in the magnetization for the PW functional found using the LMTO method and is an indication that a full-potential approach is needed in order to determine the effects of the GC's on the magnetic proper-

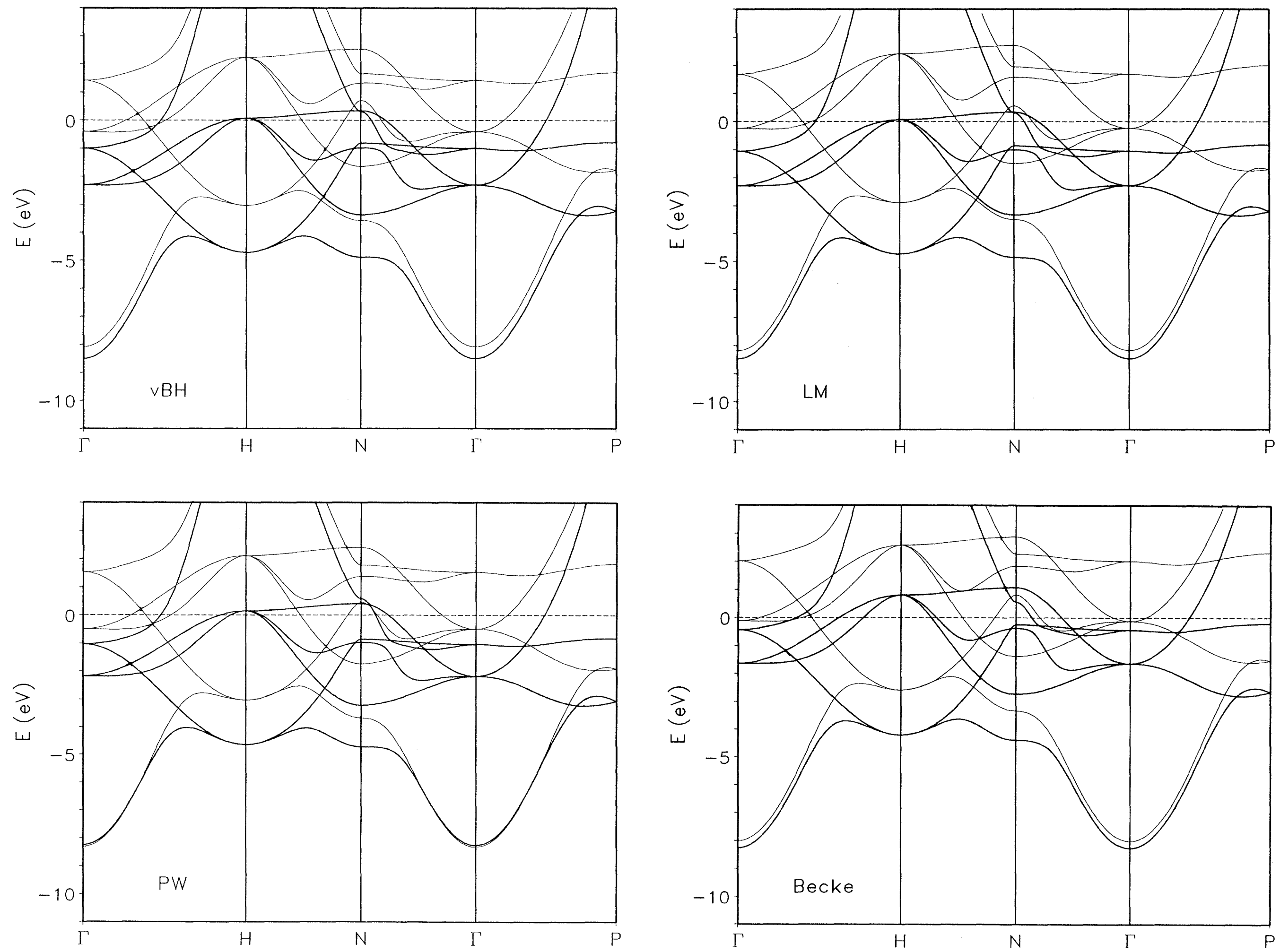

FIG. 1. Band structures for bcc iron at the experimental lattice parameter. The heavy curves are the majority spin bands while the light curves are for the minority spin.

TABLE III. Exchange splittings Δ for iron at the experimental lattice parameter with different xc functionals. The column labeled MT refers to the LSDA muffin-tin approximation augmented plane-wave calculations of Ref. 33.

			Δ (eV)		
	MT	vBH	LM	PW	Becke
Γ_1	0.276	0.419	0.294	-0.056	0.327
Γ'_{25}	1.74	1.901	2.043	1.686	1.788
Γ_{12}	1.90	2.420	2.737	2.568	2.581
$\Delta(\Gamma_{12})-\Delta(\Gamma'_{25})$	0.16	0.519	0.694	0.882	0.793
P_4	1.11	1.47	1.51	1.16	1.37
P_3	1.97	2.49	2.82	2.65	1.94

ties. As noted, the PW and Becke functionals yield reductions in the magnetization. In the case of the Becke functional, the reduction is small, yielding slightly better agreement with experiment. For the PW functional the correction is larger, yielding quite good agreement with experiment. In the case of the LM functional, the moment increases, degrading the agreement with experiment. Thus, as in the case of the structural ground-state properties, the best agreement with the experimental moment is found for the PW functional. It is significant that the magnetizations calculated using the three GC xc functionals span a wide range around the LSDA value. This large variation may be related to that found between the LM and PW GC's in atomic calculations on $3d$ atoms.[18] It is possible that more sophisticated forms of the GCLSDA functional will improve the agreement of the calculated moments with experiment. Because of the wide variation (10%) found here, this remains an open question.

Self-consistent LSDA and GCLSDA band structures at the experimental lattice parameter are shown in Fig. 1. Selected exchange splittings and eigenvalues are given in Tables III and IV. The corresponding electronic densities of states (DOS) are given in Fig. 2, with the DOS at the Fermi energy $N(E_F)$ given in Table V. It is significant that while the GCLSDA band structures are qualitatively similar to the LSDA band structures, the corrections differ considerably. For example, for the LM functional the s states are slightly lowered (by approximately 0.1 eV) relative to the d states, while with the PW functional there is only a very small relative shift of these states. In the case of the Becke functional, the s states are raised (by approximately 0.25 eV) relative to the d states. Similarly, with the LM functional the exchange splittings of the occupied Γ'_{25} state is increased over the LSDA result, while in the case of the PW and Becke functionals, this exchange splitting is reduced. Differences are also seen among the exchange splittings at P. The LSDA exchange splitting for the P_4 band agrees well with the experimental value of 1.5 eV.[35] The LM GC maintains this good agreement since it only changes this splitting by a small amount. The Becke functional reduces the splitting of this state by about 0.1 eV and thus is also in reasonable agreement with experiment. On the other hand, the PW functional seems to yield too small a splitting for this state. As may be expected from the changes in the band structure (Fig. 1), there are also significant changes in several Fermi surface areas although it is unclear whether there is any improvement in

TABLE IV. Selected majority spin band energies ϵ (relative to the Fermi energy) for iron.

		ϵ (eV)		
	vBH	LM	PW	Becke
Γ_1	-8.47	-8.45	-8.25	-8.18
Γ'_{25}	-2.27	-2.25	-2.18	-2.25
Γ_{12}	-0.96	-1.02	-1.03	-1.04
P_4	-3.20	-3.18	-3.07	-3.10
P_3	-0.75	-0.80	-0.82	-0.82

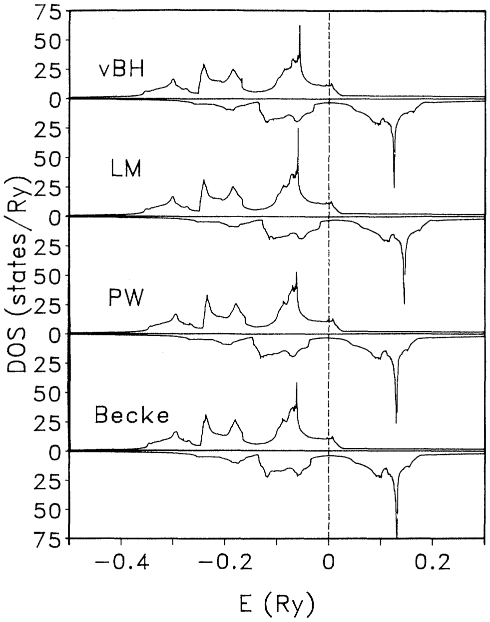

FIG. 2. Electronic DOS for ferromagnetic bcc iron. The upper curves are the calculated majority spin DOS while the lower curves are for the minority spin.

TABLE V. DOS at the Fermi energy for ferromagnetic bcc iron. $N_\uparrow(E_F)$ and $N_\downarrow(E_F)$ are the majority and minority spin DOS, respectively, in states/Ry.

	$N_\uparrow(E_F)$	$N_\downarrow(E_F)$	$N(E_F)$
vBH	11.0	3.5	14.5
LM	10.9	3.4	14.3
PW	10.8	3.3	14.2
Becke	11.2	3.7	14.9
Expt.[a]			27.37

[a]Reference 34.

the agreement with de Haas–van Alphen data.

It may be noted that all three GC functionals tested yield an increase in the exchange splitting of the Γ_{12} state. Since the minority spin component of this state is above the Fermi energy, its exchange splitting cannot be measured using photoemission. However, this enhancement of the Γ_{12} exchange splitting, and particularly the enhancement relative to the Γ'_{25} splitting by the GC's, is important. This is because these are almost pure *d* states with differing orbital characters (t_{2g} and e_g). As shown in the LSDA spin density of Fig. 3 (the GCLSDA spin densities are similar), the minority spin holes in iron reside in the e_g orbitals. Because of this, the charge density and hence the LSDA xc potential experienced by the t_{2g} orbitals differ from that experienced by the e_g orbitals. Thus it is not surprising that in a full-potential calculation, within the LSDA, the exchange splittings of the Γ_{12} and Γ'_{25} states differ. This difference is given in Table III. There is a 34% enhancement over the LSDA value of this difference if the LM xc functional is used. Larger enhancements of 53% and 70% are found for the Becke and PW xc functionals, respectively. Another effect common to the three GC's tested is a fairly substantial reduction in the exchange splitting of the *s*-like Γ_1 state. In the case of the PW functional, this splitting is effectively zero.

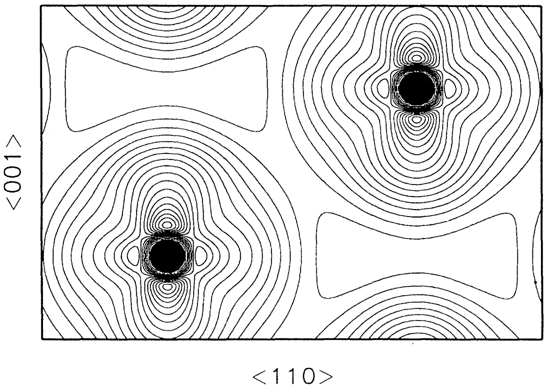

FIG. 4. Difference of the self-consistent minority and majority spin potentials for the vBH xc functional in a (110) plane. Adjacent contours are separated by 20 mRy.

GCLSDA calculations are entirely within the density-functional formalism so that the same local xc potential is used for each band. Thus it is reasonable to relate the changes found when GC's to the LSDA are incorporated to the changes in the xc potential. Since the most important changes in the electronic structure of iron are apparently related to its magnetism, we focus on the difference between the minority and majority spin potentials (referred to as the spin difference potential in the following). This difference is shown in Fig. 4 for iron in the LSDA at the experimental lattice parameter. An examination of this difference shows that, like the spin density, it is quite anisotropic even within the LSDA. Most of this anisotropy is due to the anisotropy in the minority spin potential. This in turn arises from the anisotropy of the minority spin charge density. The self-consistent spin difference potential is shown for the LM functional in Fig. 5 and the difference between this and the vBH result is shown in Fig. 6. An examination of these plots reveals that the anisotropy of the spin difference potential is enhanced by the LM GC with much of the enhancement occurring at the periphery of the *d* lobes containing the

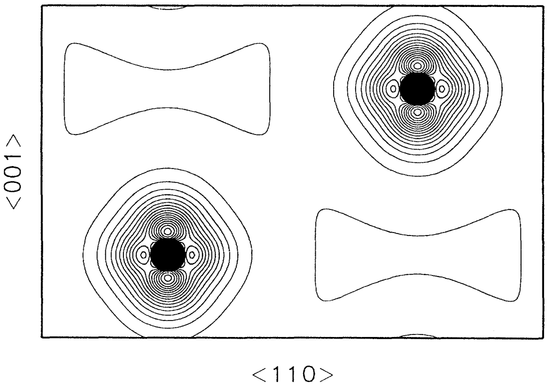

FIG. 3. (110) contour plot of the LSDA spin density for bcc iron at the experimental lattice parameter. Adjacent contours are separated by 0.05 e/a.u.^{3}.

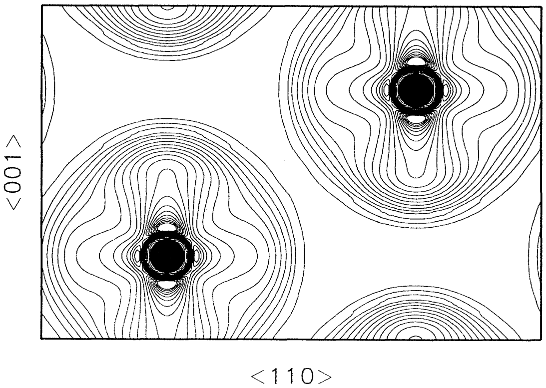

FIG. 5. Difference of the self-consistent minority and majority spin potentials for the LM xc functional in a (110) plane. Adjacent contours are separated by 20 mRy.

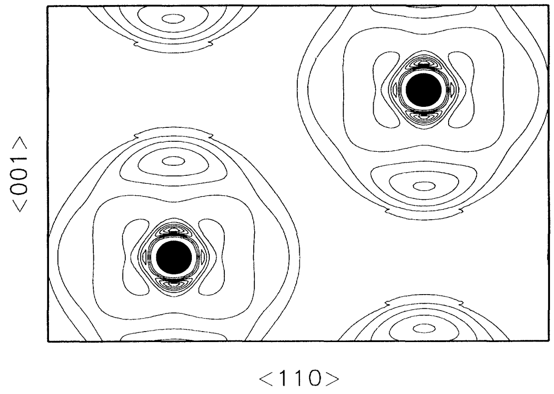

FIG. 6. Difference of the potentials of Figs. 4 and 5. Adjacent contours are separated by 20 mRy.

minority spin holes. A separate examination of the majority and minority spin potentials (not shown) indicates that this change arises from an increase in the anisotropy of the minority spin potential. The PW and Becke GC's are qualitatively similar in that they also increase the anisotropy of the spin difference potential.

In a muffin-tin approximation the exchange splitting of the Γ_{12} and Γ'_{25} states may be expected to be quite similar because they are both almost pure *d* states and lie within the MT where the potential is spherically averaged. As may be noted from the muffin-tin approximation results[31] in Table III, this is, in fact, the case. (Note that the bands at *P* have differing *s* characters and accordingly the exchange splittings of these bands differ significantly even in a MT approximation.) As noted, in full-potential LSDA calculations the charge densities and hence the xc potentials are not in general spherical, and, as shown by the present calculation, for example, this can differentiate orbitals through differences in their exchange splittings. Thus, claims that the LSDA is inherently unable to deal with anisotropic effects are in our view overstated. A more accurate statement would be that the LSDA appears to underestimate anisotropic effects in certain open-shell systems. This distinction is important because, since GCLSDA formalism is quite similar to that of the LSDA, the former statement, if true, would imply that GCLSDA is also unable to deal with anisotropic effects.

As mentioned, Kutzler and Painter[15] found that GCLSDA stabilizes nonspherical atoms, improving the agreement with experiment. Our calculations demonstrate that a similar effect occurs in iron. That is, the difference between the fully occupied orbitals and the orbitals containing the minority spin hole is enhanced and the magnetic state is stabilized relative to the nonmagnetic state.[36] Through a series of calculations in which the anisotropy of the spin difference xc potential was artificially enhanced, Singh and co-workers found that a qualitatively correct (i.e., magnetic and insulating) ground state for $CaCuO_2$ could be stabilized.[26] This result is consistent with the view that one of the important deficiencies of the LSDA in describing correlated systems arises from its inability to distinguish occupied and unoccupied orbitals in a given shell.[37] This deficiency can be overcome through the use of orbital-dependent potentials such as self-interaction corrections.[32,38] We note, however, that since different orbitals have different spatial distributions, they sample different parts of the potential. Thus, at least in principle, similar effects can be produced through anisotropic variation of the local potential. While the anisotropic fields required to yield an insulating solution for $CaCuO_2$ were several times larger than the enhancements in the anisotropy of the spin difference potentials produced by the GC's in iron, the qualitative similarity is striking. GCLSDA calculations for $CaCuO_2$ are in progress and will be reported elsewhere.

The calculated $N(E_F)$, given in Table V, indicate that none of the GC's yield a significant improvement over the LSDA result, which is approximately half the experimental value. It seems unlikely that the enhancement due to the electron-phonon interaction will entirely remove this discrepancy, since to do so would require a λ of 0.9. This is to be compared with a rigid-muffin-tin-approximation (RMTA) value of 0.52 calculated by Papaconstantopoulos and co-workers for paramagnetic iron.[39] Assuming, therefore, that ferromagnetic iron does not have an unusually large λ, it would seem that there remains a discrepancy between the calculated and experimental band masses which is not resolved by the use of GC's. This may be taken as an indication that while the use of GC's to the LSDA may improve ground-state properties and possibly the large scale aspects of band structures, it is unlikely that refinements to the GC's will improve excitation spectra near the Fermi energy significantly. This conclusion is consistent with the failure of GCLSDA to improve excitation spectra found in previous calculations for Cu, V, and some semiconductors.[19,20] It should, however, be noted that this in itself is not an indication of a breakdown of GCLSDA theory since, strictly speaking, the density-functional formalism is valid only for ground-state properties and even if the (unknown) exact density functional could be used, it is unclear whether it would yield an improvement over the LSDA excitation spectra.

CONCLUSIONS

Full-potential GCLSDA calculations for iron have been reported using the LM, PW, and Becke forms of the xc functional. In all three cases the effect of the GC's is to stabilize the ferromagnetic bcc phase through an increase in the magnetic energy. The calculated magnetic moments and exchange splittings differ between the different functionals, with the LM functional often correcting the LSDA values in the opposite direction of the PW functional. The best overall agreement with experimental *ground-state* properties was found for the PW functional. On the other hand, the LM functional seems to give better exchange splittings for iron. Clearly, more work to determine the optimum form of the GC is required. Significantly, for all three forms of the GC tested, the anisotropy of the xc potential is increased over the LSDA result.

ACKNOWLEDGMENTS

Two of us (D.S. and W.E.P.) were supported by the Office of Naval Research. One of us (H.K.) was supported in part by the National Science Foundation through Grant No. DMR-87-19535. Computations were performed at the Cornell National Supercomputer Facility. D.S. is pleased to acknowledge several helpful discussions with Baird Brandow, Axel Svane, D. A. Papaconstantopoulos, and M. J. Mehl. W.E.P. acknowledges illuminating discussions with Baird Brandow and with Rex Godby, T. Jarlborg, Elio Moroni, and Gerardo Ortiz during a stay at the Ecole Polytechnique Federale de Lausanne. W.E.P. is also grateful for the hospitality of the Cavendish Laboratory during the completion of this paper.

---

[1] C. S. Wang, B. M. Klein, and H. Krakauer, Phys. Rev. Lett. **54**, 1852 (1985).

[2] K. B. Hathaway, H. J. F. Jansen, and A. J. Freeman, Phys. Rev. B **31**, 7603 (1985); H. J. F. Jansen, K. B. Hathaway, and A. J. Freeman, *ibid.* **30**, 6177 (1984).

[3] H. J. F. Jansen and S. S. Peng, Phys. Rev. B **37**, 2689 (1988).

[4] J. Chen, D. Singh, and H. Krakauer, Phys. Rev. B **37**, 2689 (1988).

[5] W. Borgiel and W. Nolting, Z. Phys. B **78**, 241 (1990); W. Borgiel, W. Nolting, and M. Donath, Solid State Commun. **72**, 825 (1989); W. Nolting, W. Borgiel, V. Dose, and Th. Fauster, Phys. Rev. B **40**, 5015 (1989), and references therein.

[6] J. M. MacLaren, D. P. Clougherty, and R. C. Albers, Phys. Rev. B **42**, 3205 (1990). In this reference it is shown that the particular spin interpolation used in the LSDA can shift the fcc-bcc energy difference for iron. Full-potential calculations indicate that this shift is too small to yield a bcc ground state [D. J. Singh and C. S. Wang (unpublished)].

[7] J. A. Alonso and L. A. Girifalco, Phys. Rev. B **17**, 3735 (1978).

[8] O. Gunnarsson, M. Jonson, and B. I. Lundqvist, Phys. Rev. B **20**, 3136 (1979).

[9] J. P. Perdew, Phys. Rev. Lett. **55**, 1665 (1985), and references therein.

[10] D. C. Langreth and M. J. Mehl, Phys. Rev. Lett. **47**, 446 (1981); C. D. Hu and D. C. Langreth, Phys. Scr. **32**, 391 (1985).

[11] J. P. Perdew and W. Yue, Phys. Rev. B **33**, 8800 (1986); J. P. Perdew, *ibid.* **33**, 8822 (1986); **34**, 7406(E) (1986).

[12] A. D. Becke, Phys. Rev. B **38**, 3098 (1988).

[13] D. C. Langreth and M. J. Mehl, Phys. Rev. B **28**, 1809 (1983).

[14] A. D. Becke, J. Chem. Phys. **84**, 4524 (1986).

[15] F. W. Kutzler and G. S. Painter, Phys. Rev. B **37**, 2850 (1988); Phys. Rev. Lett. **59**, 1285 (1987); there appears to be a misprint in Eq. (4). There should be a minus sign on the second line preceding the bracket which follows the $(2-F)\nabla^2 n(\mathbf{r})$.

[16] G. Ortiz and P. Ballone, Phys. Rev. B **43**, 6376 (1991).

[17] A. Savin, U. Wedig, H. Preuss, and H. Stoll, Phys. Rev. Lett. **53**, 2087 (1984).

[18] J. B. Lagowski and S. H. Vosko, J. Phys. B **21**, 203 (1988).

[19] M. R. Norman and D. D. Koelling, Phys. Rev. B **28**, 4357 (1983).

[20] X. J. Kong, C. T. Chan, K. M. Ho, and Y. Y. Ye, Phys. Rev. B **42**, 9357 (1990).

[21] P. Bagno, O. Jepsen, and O. Gunnarsson, Phys. Rev. B **40**, 1997 (1989).

[22] B. Barbiellini, E. G. Moroni, and T. Jarlborg, J. Phys. Condens. Matter **2**, 7597 (1990).

[23] M. Rasolt and H. L. Davis, Phys. Lett. **86A**, 45 (1981); M. Rasolt, Phys. Rev. B **16**, 3234 (1977); a direct gradient expansion was used for the spin interpolation, similar in spirit to the work of Ma and Brueckner (Ref. 24) for the paramagnetic electron gas. This is in contrast to the generalized expansions used in modern GCLSDA functionals.

[24] S.-K. Ma and K. A. Brueckner, Phys. Rev. **165**, 18 (1968).

[25] A. M. Oles and G. Stollhoff, Phys. Rev. B **29**, 314 (1984).

[26] D. Singh, W. E. Pickett, R. E. Cohen, D. A. Papaconstantopoulos, and H. Krakauer, Physica B **163**, 470 (1990); D. Singh, W. E. Pickett, and H. Krakauer, Physica C **162-164**, 1431 (1989).

[27] O. K. Andersen, Phys. Rev. B **12**, 3060 (1975); D. R. Hamann, Phys. Rev. Lett. **42**, 662 (1979); E. Wimmer, H. Krakauer, M. Weinert, and A. J. Freeman, Phys. Rev. B **24**, 864 (1981); S.-H. Wei and H. Krakauer, Phys. Rev. Lett. **55**, 1200 (1985); S.-H. Wei, H. Krakauer, and M. Weinert, Phys. Rev. B **32**, 7792 (1985).

[28] D. J. Singh, Phys. Rev. B **43**, 6388 (1991); the basis denoted SLAPW-3 extended to all angular momenta was used in the present study.

[29] F. D. Murnaghan, Proc. Nat. Acad. Sci. U.S.A. **30**, 244 (1944).

[30] A. Baldereschi, Phys. Rev. B **7**, 5212 (1973); D. J. Chadi and M. L. Cohen, *ibid.* **8**, 5747 (1973); H. J. Monkhorst and J. D. Pack, *ibid.* **13**, 5188 (1976); **16**, 1748 (1977).

[31] U. von Barth and L. Hedin, J. Phys. C **5**, 1629 (1972).

[32] J. P. Perdew and A. Zunger, Phys. Rev. B **23**, 5048 (1981).

[33] D. A. Papaconstantopoulos, *Handbook of the Band Structure of Elemental Solids* (Plenum, New York, 1986), pp. 95–102.

[34] M. Dixon, F. E. Hoare, T. M. Holden, and D. E. Moody, Proc. R. Soc. London Sec. A **285**, 561 (1965); note that the enhancement due to the electron-phonon coupling is included in the experimental value but not the calculated band-structure values (see text).

[35] D. E. Eastman, F. J. Himpsel, and J. A. Knapp, Phys. Rev. Lett. **44**, 95 (1980).

[36] The stabilization of the magnetic state cannot be ascribed in its entirety to the enhanced asphericity in the GCLSDA calculations, since a stabilization is also found in the LMTO calculations of Refs. 20 and 21.

[37] For a discussion of this and other deficiencies of the LSDA in Mott insulators, see B. Brandow, in *Narrow-Band Phenomena-Influence of Electrons with both Band and Localized Character,* edited by J. C. Fluggle, G. A. Sawatzky, and J. W. Allen, (Plenum, New York, 1988), p. 97; B. Brandow, Int. J. Quantum Chem. Symp. **10**, 417 (1976).

[38] A. Svane and O. Gunnarsson, Phys. Rev. Lett. **65**, 1148 (1990).

[39] D. A. Papaconstantopoulos, L. L. Boyer, B. M. Klein, A. R. Williams, V. L. Morruzzi, and F. J. Janak, Phys. Rev. B **15**, 4221 (1977); as discussed in this reference, the RMTA probably results in an overestimate of λ, with a value of 0.27 being more realistic.